Proceedings of Symposium on Ultrasonic Electronics, Vol. 30 (2009) pp. 107-108
18-20 November, 2009

FEM Analysis of Sound Field Characteristics in Air Gaps of Noncontact Ultrasonic Motor with Flexural Standing Wave Vibration Disks

定在波屈曲振動円板を用いた非接触超音波モータのギャップ内音場特性の有限要素法解析

Yasuhiro Yamayoshi†, Jun Shiina, Hideki Tamura and Seiji Hirose
(Facult. Eng., Yamagata Univ.)
山吉康弘†，椎名潤，田村英樹，広瀬精二 （山形大 工）

1. Introduction

Recently, we proposed a new noncontact ultrasonic motor with two flexural standing wave vibration disks [1]. In this paper, we investigate the relationship between the experimental revolution speed characteristics and the sound field characteristics in the air gaps analyzed by FEM.

2. Construction of motor

Figure 1 shows the construction of the noncontact ultrasonic motor with two flexural standing wave vibration disks. The disk rotor with a 25 mm diameter (D_r) and a 2 mm thickness (t_r) is sandwiched between two pairs of an air gap and a disk stator, and is not in contact with both stators. The rotor rotates together with a central shaft supported by two ball bearings and one pivot tip. The stators are fixed with the differential angle $\Delta\theta$ by which the stator-II is twisted in the circumferential direction from the same position as the stator-I. Moreover, the two stators are driven by two voltages, where the temporal phases of each voltage for the stator-I and stator-II are ϕ_1 and ϕ_2, respectively. $\Delta\phi$ is defined as the phase difference ϕ_2 - ϕ_1 between the voltages applied to the two stators. The stator is composed of a vibration disk and a support ring that are produced from one aluminum plate of 0.4 mm thickness. The six thin bars extended along the nodal lines of the vibration connect the vibration disk and support ring. A lead zirconate titanate (PZT) disk with a 0.15 mm thickness, which is polarized in the thickness direction, is bonded to the vibration disk with a 30 mm outer diameter (D_s) and a 1 mm inner diameter. Six fan-shaped electrodes for inducing a flexural standing wave vibration mode called the B_{13} mode are formed on the surface of the PZT disk.

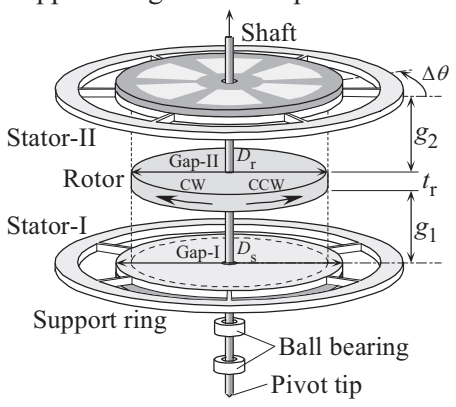

Fig. 1 Construction of noncontact ultrasonic motor with flexural standing wave vibrating disks.

yamayosi@yz.yamagata-u.ac.jp

3. FEM analysis of sound field characteristics

Figure 2 shows the model for FEM analysis. The support ring and the connected bars are neglected from the model for simplification. The acoustic elements of air are added to around the two stators and the rotor. The analysis is conducted using the one third section model of a cylinder which is given the periodical boundary condition of 120° unit and the the perfectly absorptive boundary condition at the surfaces. In the FEM (ANSYS 11.0) used in this analysis, the interaction between

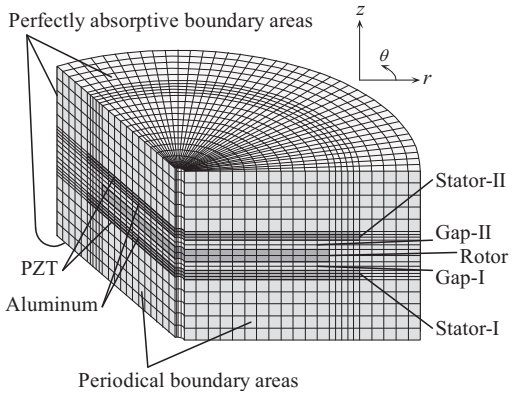

Fig. 2 Model for FEM analysis.

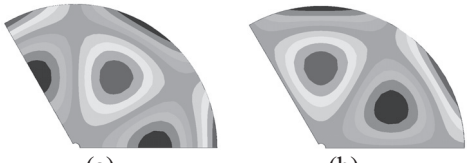

(a) (b)

Fig. 3 Vibration displacement patterns of (a) stator-I and (b) stator-II. (Top view)

piezoelectric materials, structures, and acoustic elements is considered, but the viscous of air is not considered. **Figure 3** shows the vibration displacement patterns of the stator-I and stator-II. The pattern of stator-II is shifted in the θ direction by -30° from the pattern of the stator-I. In this analysis, both gap distances of g_1 and g_2 are set in 0.5 mm.

Figure 4 shows the calculated results of the sound pressure in the r direction at the position of θ = 0°. The voltages out of phase ($\Delta\phi$ = 90°) with a same amplitude are applied to the two stators. The sound pressures, normalized by the maximum value, on the same z position as the lower and upper surface of the rotor are illustrated as gap-I and gap-II. The outline positions of the stator and the rotor are indicated by the solid and broken straight lines in this figure. The intense sound pressures with the same amplitude distribution are mainly generated in the two air gaps but the slight acoustic leaks arise at the outside of the air gaps. **Figure 5** shows the sound pressure in the θ direction at the position of r = 8.5 mm. The amplitude of sound pressure is nearly constant but the phases differ by about 180° and are almost proportional to θ. It has been clarified that the acoustic traveling waves having the reverse phase and the same traveling direction occure in the two air gaps. **Figure 6** shows the standing wave ratio of the sound pressure (SWR) in the two air gaps as a function of $\Delta\phi$. The SWR is the value which divided the maximum value by the minimum value of the sound pressure at the position of r = 8.5 mm. When the voltages in phase are applied to the two stators, the sound fields of the standing wave are generated in the air gaps. The nearer to 90° the $|\Delta\phi|$ is, the more the sound fields approach to the traveling wave of SWR ≈ 1. The sound fields travel in the CCW and CW direction according to the negative and positive $\Delta\phi$, respectively. In the calculated results of $\Delta\theta$ = +30°, the traveling direction of the sound fields are opposite to the result shown in Fig. 6. The traveling direction of the sound fields coincides with the rotation direction of the rotor which has been observed in the experiments [1]. We consider that when the standing wave sound fields are generated in the air gaps, the rotor does not rotate and when the sound fields in the air gaps are nearer to the complete traveling wave, the rotor rotates at the higher revolution speed. In the analysis results that the voltage is applied to only the one stator, the standing wave sound fields out of phase by about 180° are generated in the two air gaps. The traveling wave sound fields in the two air gaps are expected to be formed by the superposition of the standing wave sound fields generated by the two stators whose temporal phase and spatial position differ.

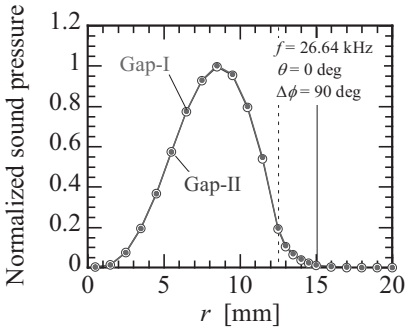

Fig. 4 Normalized sound pressure in radial direction.

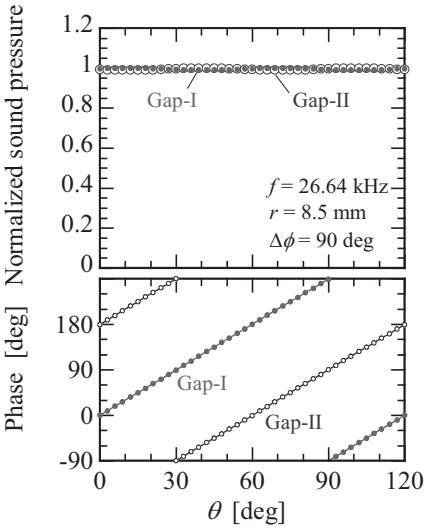

Fig. 5 Normalized sound pressure and phase in circumferential direction.

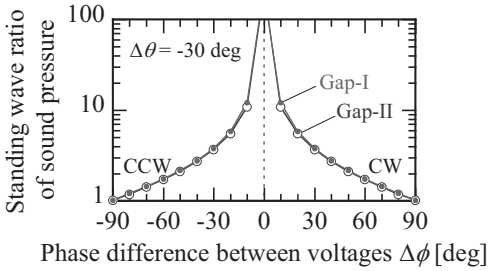

Fig. 6 Standing wave ratio of sound pressure as a function of phase difference between applied voltages.

4. Conclusion

The traveling direction of sound fields in the two air gaps analyzed by FEM has coincided with the rotation direction of rotor which has been observed in the experiments.

Acknowledgment

This work was partially supported by a Grant-in-Aid for Scientific Research (21920022) from the Japan Society for the Promotion of Science (JSPS).

Reference

1. Y. Yamayoshi, J. Shiina, H. Tamura, and S. Hirose: Proc. of The 26th Meeting on Ferroelectric Materials and Their Applications, 29-P-8, pp. 101-102, 2009.